



# Earthquake disaster map using GIS analysis: a case study of Bener Meriah-Aceh, Indonesia

Ahmad Farhan<sup>1</sup> · Abdillah Imron Nasution<sup>2</sup> · Akhyar<sup>3</sup>

Received: 13 December 2022 / Accepted: 24 December 2023 / Published online: 11 January 2024  
© Saudi Society for Geosciences and Springer Nature Switzerland AG 2024

## Abstract

This study aimed to analyze earthquake disaster risk based on the Bener Meriah-Aceh map in Indonesia, specifically focusing on the event that occurred on July 2, 2013, measuring 6.2 on Richter scale with a significant impact on both society and the environment. The method used was Geographic Information System (GIS), a technique for disaster analysis. Earthquake disaster map which was produced by referencing the Indonesian law for disaster map standard (Perka BNPB 2/2012) was analyzed using an overlay of three components, namely, hazard, vulnerability, and capacity. Furthermore, the generation of earthquake hazard map involved the collection of some data, such as the SNI earthquake map (Indonesia National Standard), the length of an active fault, ten years of MMI (Modified Mercalli Intensity) map, fault density, and geomorphology and geology maps. Vulnerability earthquake map was obtained by analyzing the physical, economic, and social hazard data, while capacity map was calculated using the indicator in the Hyogo Framework for Actions. The results showed that 122 people were exposed to the low-level earthquake risk, with 37,768 belonging to the threatened vulnerable group, leading to physical-economic losses of IDR 368 billion (Indonesian Rupiah). In the medium category, 1869 people were exposed, and 48,809 were potentially vulnerable, resulting in physical-economic losses of IDR 718 billion. Perka BNPB 2/2012 states that the exposed victims were directly impacted in the risk area (low-medium-high). The vulnerable group comprises children under 5, the elderly, people with disabilities, and individuals living in poverty within the analyzed districts. Therefore, earthquake disaster risk analysis for the Bener Meriah district yielded two categories, namely, medium and low.

**Keywords** Earthquake · Disaster · Hazard · Vulnerability · Capacity · GIS

## Introduction

Earthquake disaster risk map was selected for analysis in the Bener Meriah district due to the significant impact of the event which occurred on July 2, 2013, measuring 6.2 on the Richter scale. The effect of this earthquake was damage to houses and infrastructure, landslides, and displacement of

the local population. Recent studies in Dhaka City, Bangladesh, used GIS tools to produce earthquake vulnerability map. During this process, the physical and socio-economic data of the quantitative sample were analyzed by GIS shapefiles (Rahman et al. 2015). Another similar study assessed the seismic hazard in north-western Egypt using a probabilistic method. To develop the seismicity model, the seismic sources were delineated, and the seismicity parameters were determined (Ezzelarab et al. 2016). A study focused on an uncertainty assessment of new seismic hazard map in Spain, employing various phases for the probabilistic seismic hazard evaluation (Gaspar-Escribano, al., 2015). The post-disaster analysis of the local impact of the destructive earthquake with a magnitude of 7.6 scales in northern Pakistan on October 8, 2005, was reported in a relevant study (Halvorson and Hamilton 2010).

A total of two algorithms were applied for the immediate rectification of unified images in earthquake disaster area without the need for control points, using an

---

Responsible Editor: Longjun Dong

✉ Akhyar  
akhyar@usk.ac.id

<sup>1</sup> Department of Physical Education, FKIP Universitas Syiah Kuala, Darussalam, Banda Aceh 23111, Indonesia

<sup>2</sup> Department of Oral Biology, Faculty of Dentistry, Universitas Syiah Kuala, Banda Aceh 23111, Indonesia

<sup>3</sup> Department of Mechanical Engineering, Universitas Syiah Kuala, Jl. Syech Abdurrauf No. 7, Darussalam, Banda Aceh 23111, Indonesia

unmanned aerial vehicle (UAV) system (Chang-chun et al. 2011). Pilot studies were conducted in the metropolitan area of Tokyo on earthquake vulnerability by considering various aspects, such as the physical environment, the number of people at risk, the economic dimension, and social vulnerability with GIS analytical tools (Uitto 1998). To examine earthquake disaster on an urban scale, an integrated urban seismic simulation system was developed, using GIS, computer-aided design (CAD), finite element analysis (FEA), and virtual reality (VR) as a model of numerical simulation (Feng et al. 2008). The distribution analysis for emergency evacuation, accessibility to shelter, and optimization of the evacuation objectives were applied by Ye et al. (2012). Furthermore, employed GIS technique to analyze disaster prevention and mitigation. The Haiti earthquake case study was described in connection with the web-based mapping services, namely, CrisisCamp Haiti, OpenStreetMap, Ushahidi, and GeoCommons (Zook et al. 2010). The experiences of stakeholders in enhancing GIS capacity for disaster risk reduction in low- and middle-income countries were explored, alongside theoretical concepts of disaster risk reduction (DRR) (Rürup and Charlin 2017). The recovery efforts of the Mid-Niigata and Chuetsu-Oki earthquake in October 2004 and July 2007 were studied using social survey and GIS spatio-temporal analysis (Kimura et al. 2015). Finally, GIS tool was used to facilitate seamless interaction between disaster management and daily operations, aiming to build disaster-resilient societies (Urakawa 2016).

Numerous models, applied through GIS tools employing overlay, scoring, and AHP analysis, have been documented in recent literature. The GIS overlay score method has been utilized for analyzing infiltration rates and assessing factors that govern groundwater recharge potential (Abdelkarim et al. 2022). Analytical hierarchy process (AHP) and hydrogeological and hydrochemical methods have been employed to evaluate the suitability of irrigation water (Abdelkarim et al. 2023). Reports have detailed physicochemical elements and various factor categories, encompassing hydrogeologic, geomorphologic, and geologic considerations (Missaoui et al. 2022). Drought characteristics and propagation, including the steady-state probability of drought events and the mean duration for each station, were investigated using the Standardized Precipitation Index, Standardized Groundwater Level Index, first-order Markov chain model, and wavelet transform (Yeh and Hsu 2019). The hydrogeochemical characteristics of groundwater quality for irrigation were assessed through principal component analysis, the analytical hierarchy process (AHP) method in conjunction with GIS, revealing short-term variations under various impact variables (Missaoui et al. 2023). Artificial neural networks

and stochastic time series were employed by Agoubi and Kharroubi (2019) to study short-term impacts.

The government and stakeholders in Bener Meriah have an urgent need for earthquake disaster map which would be used as a reference to mitigate more significant damages and decrease the higher number of victims. Furthermore, it plays a vital role in regional development planning, aiming to minimize the number of victims, as well as reduce physical and economic destructions. In this study, the application of GIS as a tool for mapping earthquake disaster was discussed, specifically using the Perka BNPB No. 2 in 2012 (Indonesia Regulation from National Disaster Bureau). This regulation has previously been employed to develop tsunami disaster risk map (Farhan and Akhyar 2017). Therefore, this study aimed to evaluate earthquake disaster in the Bener Meriah District, Aceh Province, Indonesia, by employing GIS tool for disaster analyses and using the Perka BNPB 2/2012 as a baseline reference. Both the regional government and stakeholders require this map for better planning and development synergy with disaster management efforts. There is a lack of previous studies specifically discussing the systematic implementation of Perka BNPB 2/2012 for analysis of disaster risk map in Indonesia. This is because the regulation serves as a reference rule for producing risk map in the country.

## Materials and methods

### Study area

The Bener Meriah District with Simpang Tiga Redelong as its capital has an area of 1941.61 km<sup>2</sup>. Furthermore, it was located in the north of Aceh, surrounded by the North Aceh and Bireuen District, Aceh Tengah District in the south, East Aceh District in the east, West Aceh District in the west, and Aceh Tengah District in the south. The coordinates of the Bener Meriah district were N 4°33'50"–N 4°54'50" and E 96°40'75"–E 97°17'50", and the altitude ranged from 100 to 2500 masl (meter above sea level). The population size of the district was 128,538 people, residing in ten sub-districts and 233 villages. The map of the study area in Bener Meriah District is shown in Fig. 1.

### Data set

For vulnerability analysis, the attribute data source was obtained in tabular format from the BPS (Indonesia Statistical Institution). During the preparation of vulnerability and capacity map, the attribute data were verified and corrected at the district level. The base map, which included the topographic information, such as administrative boundaries, roads, rivers, and contours, was obtained from the BIG

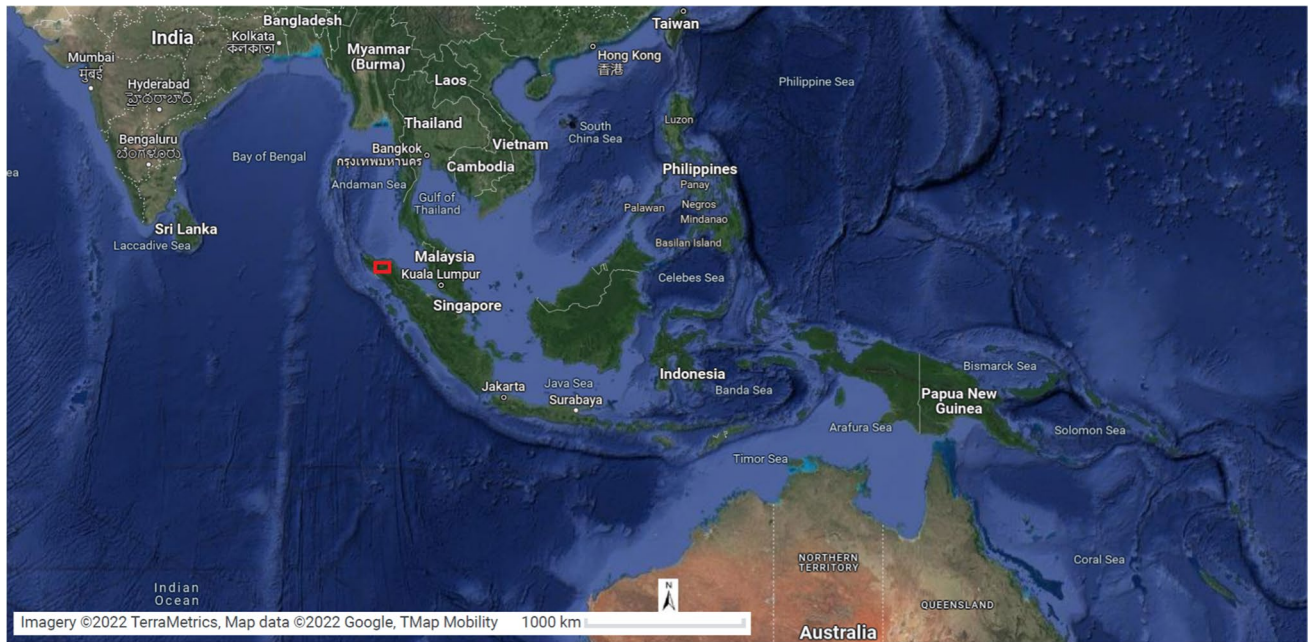


**Fig. 1** Study area map

(Indonesia Geospatial Institution). Additionally, spatial data for general venue locations were updated through field surveys conducted using GPS (Geographic Positioning System) devices.

The population density, sex ratio, poverty ratio, disabled people ratio, and age group ratio were obtained from the Statistical Bureau (BPS). The economic vulnerability was determined from the scoring of productive land use and PDRB (gross domestic product). To evaluate physical vulnerability, the numbers of houses, public facilities, and critical facilities were calculated. Earthquake hazard map and the SNI (National Indonesia Standard) version were obtained from the Indonesia Earthquake Map Revision Team, commonly known as Tim-9, which was generated under the coordination of the Department of Public Works. The geologic map used in this analysis was acquired from the Geology Bureau. Additionally, earthquake intensity map (MMI) was provided by the BMKG (Meteorology Climatology Geophysics Bureau), and the fault active data set was obtained from the Geology Bureau.

The active Sumatra tectonic system's primary folds and faults are aligned northwest to southeast, as shown in Fig. 2. Along the coastal plain's eastern edge, compressional or transpressional structures appear when the deformation intensity decreases. The Australian and Asia Plates are converging at an oblique angle during subduction, which causes a right-lateral offset along the Bukit Barisan strike-slip faults (Wardhana et al. 2023).

Figure 3 shows the seismicity of Indonesia and its nearby regions from January 1, 2000, to July 28, 2020, for all events

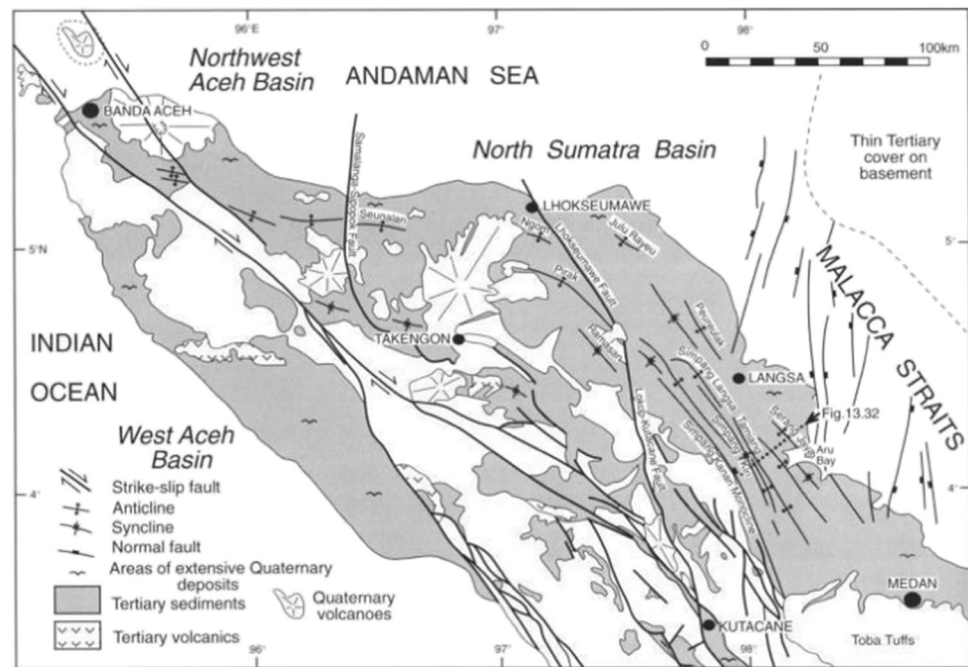
(Fig. 3a)  $\geq M$  4.6 and (Fig. 3b)  $\geq M$  7.0 (U.S. Geological Survey, 2020). Most occurrences are shallow, are clustered close to plate boundaries, and have a relatively low magnitude ( $< M$  6.0). Events  $\geq M$  7.0 are not unusual. Hypocenters are magnitude-scaled and depth-colored. Table 1 provides more details on the noteworthy occurrences marked in panel (Fig. 3b) (Hutchings et al. 2021).

### Data analysis

Disaster risk map was prepared with a semi-quantitative method which involved weighting factors and index values. This method draws an analogy to the Human Development Index (HDI), where the index value was converted to a score between 0 and 1, which indicated values from lowest to highest. The indexes 0 and 1 identify the minimum rate and maximum values of the original indicator. For regions with low numbers, logarithmic conversion was applied instead of direct conversions. Mapping analysis was performed using GIS with an overlay method, employing two databases, namely, vector and grid. The primary data were stored in a vector format, while index data was analyzed in a grid format.

The IDW (inverse distance weighting) method estimates values at specific locations based on known values from neighboring locations. This method is employed by BNPB Indonesia to generate disaster maps for the country. IDW is a spatial interpolation method utilized in the production of these maps. Interpolation methods are frequently used to estimate values in unsampled locations based on

**Fig. 2** Active tectonics in Sumatra (Wardhana et al. 2023)



measurements taken at sampled locations. The choice of interpolation method is influenced by the type of data and the geographical variability of the phenomenon under study. Here are a few interpolation techniques commonly employed in disaster maps: inverse distance weighting (IDW), kriging, spline, and radial basis function (RBF) interpolations (Perka BNPB 2/2012) (BNPB 2012).

Utilizing the IDW method, we predict unknown values at unsampled locations based on the values at sampled locations, assigning greater influence to closer samples than those further away. The spatial dataset includes  $x$ ,  $y$  (latitude-longitude), and  $z$  coordinates for evaluation. The process involves determining parameters, specifically the power and the number of neighbors ( $k$ ) for interpolation, establishing a spatial grid, calculating distances, performing weight calculations, and calculating the predicted value at each grid point using the IDW formula. The spatial results of this dataset represent the estimated values of the variables studied across the entire study area. Subsequently, validation is conducted to enhance the accuracy of predicting unknown values. The study area results reveal spatial data with either high or low predictive value and consider any spatial patterns or trends. For every sampled point in the dataset, find the distance to the target point at coordinates  $(X_i, Y_i)$ . A metric like the Euclidean distance can be used to compute the distance. Based on their distances, assign the sampled points weights. Using these weights, compute the weighted average of the variable of interest at the sample points. The interpolated value for the variable of interest at the target point  $(X_i, Y_i)$  produced by the IDW method is the computed predicted value (Yanto et al. 2022).

## Disaster risk map

Disaster risk map is an overlay of hazard, vulnerability, and capacity map. The scenario of disaster risk assessment study is presented in Fig. 4.

The risk mapping methodology can be analyzed through GIS techniques. Maps of hazard, vulnerability, capacity, and risk indexes were produced using GIS by converting vectors to a grid of raster format, as presented in the following procedure (Perka BNPB 2/2012) (BNPB 2012):

1. Creating a grid (from vector sources)
2. Merging and cutting the grid layer
3. Using color range definition for color grids and legends
4. Analyzing the specific grids (slope grids, "object distance" grids, etc.)
5. Calculating the grids
6. Classifying and reducing the grids on the contours of the grid layer
7. Preparing a statistical summary

GIS tool as one of the geospatial methodologies can be used for disaster analysis (Perka BNPB 2/2012) (BNPB 2012). Earthquake disaster maps were analyzed from an overlay of three component maps, namely, hazard, vulnerability, and capacity. To produce earthquake disaster map for Bener Meriah District, the primary reference used was Perka BNPB 2/2012, which serves as the Indonesian law governing the principle for generating disaster map standard. Hazard map was obtained through the scoring of earthquake by SNI (Indonesia National Standard), a length of active fault, ten

**Fig. 3** Indonesia’s dense seismic activity: (a) all events  $\geq M$  4.6 and (b) all events  $\geq M$  7.0 (Hutchings et al. 2021)

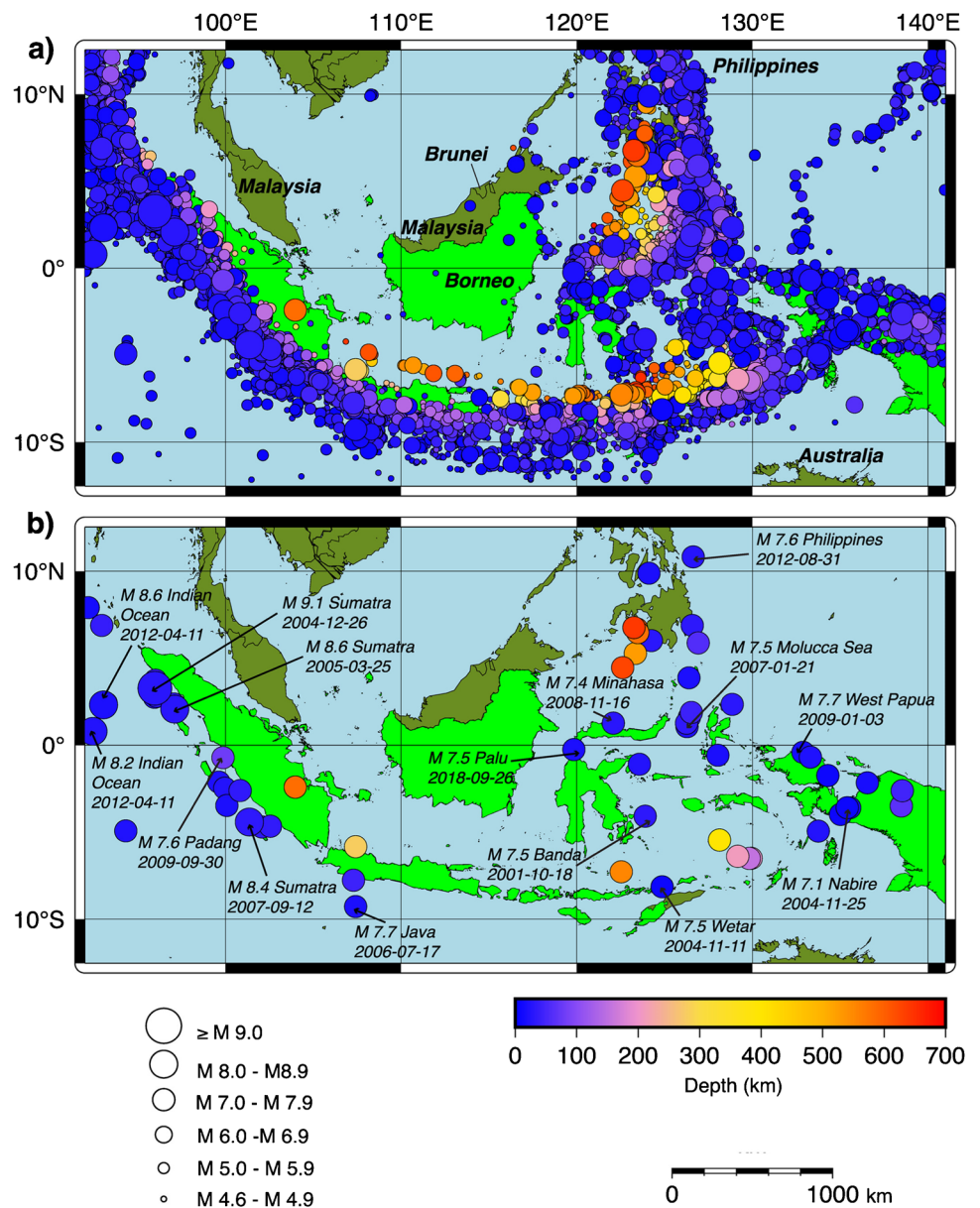


**Table 1** Number of earthquakes (Indonesia) (Hutchings et al. 2021)

Depth range (km)	Events	Percentage (%)
All	20,622	100
Shallow (0–70)	15,970	77,4
Intermediate (70–300)	4,073	19,8
Deep (> 300)	579	2,8

years MMI map (earthquake intensity), fault density, and geomorphology and geology map. Vulnerability map was created by scoring the physical facilities, economics, and social vulnerability map of Bener Meriah District.

Capacity map was calculated using the indicator in Hyogo Framework for Actions (Fariza et al. 2017). All

the weighting factors used for analysis of earthquake map (hazard and vulnerability map) were the results of the AHP process (analytical hierarchy process). To calculate the value of disaster risk, Eq. 1 was applied. The risk map has been prepared based on the index grid on hazard, vulnerability, and capacity map, following the Risk = Hazard \* (Vulnerability/Capacity) formula. To address potential issues with high or low capacity values, or errors resulting from zero values, a modification was introduced to the formula. Instead of dividing by Capacity (C), the multiplication was performed by the inverse capacity (1—C) to ensure a smoother calculation. Additionally, to revert to the original dimension, the result of the multiplication index should be corrected to the power of 1/n ( $0.25 * 0.25 * 0.25 = 0.015625$ , corrected:  $0.015625^{(1/3)} = 0.25$ ).

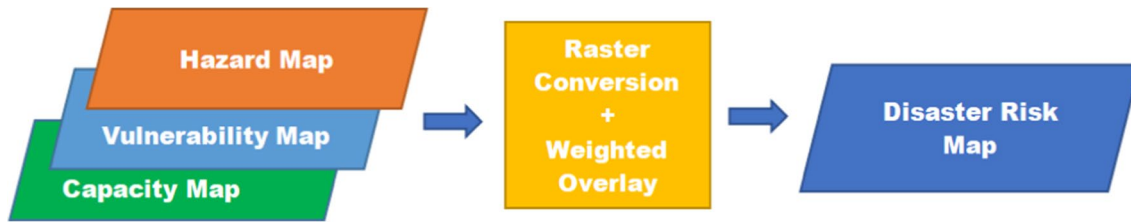


Fig. 4 Schematic representation of the methodology taken to describe earthquake disaster risk map

Equation 1 was obtained based on these corrections (Perka BNPB 2/2012) (BNPB 2012).

$$\text{Risk} = \sqrt[3]{\text{Hazard} * \text{Vulnerability} * (1 - \text{Capacity})} \quad (1)$$

Mapping analysis involved the combination of vector and grid-based GIS layers. The data was mainly stored using vector structures, while indexes were generated in a grid format. The AHP was a measurement methodology through pair-wise comparison. This process relied on expert judgment to establish a priority scale that measures in relative terms. The comparisons were made using an absolute rating scale, representing the extent an indicator dominates another concerning a particular disaster.

**Hazard map**

Each parameters used in preparing the hazard map was scored based on percentage (Fig. 5). Subsequently, earthquake hazard level of an area was used for the preparation of hazard map. Equation 2 presents analysis formula.

Hazard index was computed based on two main components, namely, the possibility of hazard and the magnitude of the impacts observed from past disaster. This index was based on historical data and records of the events that occurred within a region. The new mapping area was implemented after all the indicator data on each component were obtained. Once the necessary data were collected, they were divided into the three hazard classes of low, medium, and high.

$$\text{EHI} = (\text{SNI} * 0.4) + (\text{G1} * 0.1) + (\text{MMI} * 0.2) + (\text{F} * 0.2) + (\text{Gm} * 0.05) + (\text{FD} * 0.05) \quad (2)$$

In Eq. 2 (Perka BNPB 2/2012) (BNPB 2012), the EHI was earthquake hazard index, SNI was the Indonesian standard for earthquake map, G1 was a geology map, and MMI was the modified Mercalli intensity. Additionally, F represented the distance from an active fault (kilometers), Gm referred to the geomorphology map, and FD was a fault density. The geological map of the study area for Bener Meriah Sub-district, Aceh Province, Indonesia, is shown in Fig. 6.

A peak ground acceleration (PGA) represents the maximum ground acceleration recorded at a specific location during earthquake, and it is the number of the absolute acceleration amplitude on the accelerogram. Its spatial data for Bener Meriah District was presented in polygon shape, with the unit in square kilometers. The polygon data consisted of the three scores, such as low (PGA value < 0.2501), medium (PGA value 0.2501–0.70), and high (PGA value > 0.70). Furthermore, the distance to the active faults was represented in polygons data (km<sup>2</sup>). This data was converted from lines (unit km) to polygons (km<sup>2</sup>) using a buffering tool. The buffering polygons were classified into three scores of low (the fault line distance about 0–10,000 m), medium (5000 m), and high (10 m). The MMI scale was used to measure earthquake strength, and it was divided into 12 levels of damage caused. Additionally, the spatial data for Bener Meriah District was in polygon format, and it was attributed to the three scores, such as low (< 4 MMI), medium (4–7 MMI), and high (> 7 MMI). The geomorphology spatial layer was polygon-shaped, and its map consisted of low (hills, mountains), medium (alluvial plain, meander path), and height (flood plain, valley

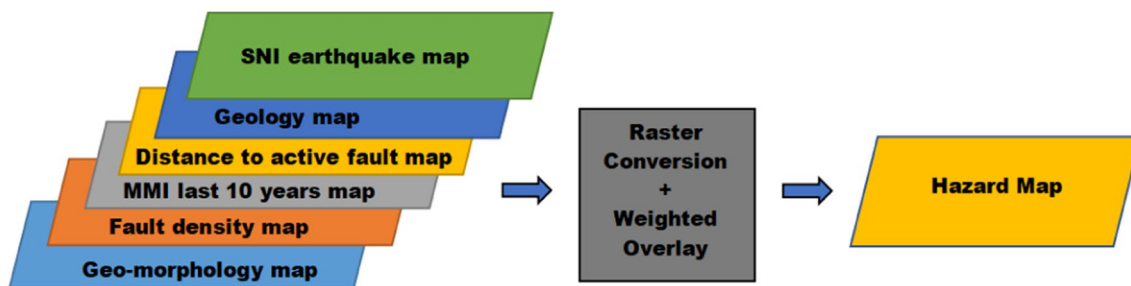


Fig. 5 Preparation of hazard map

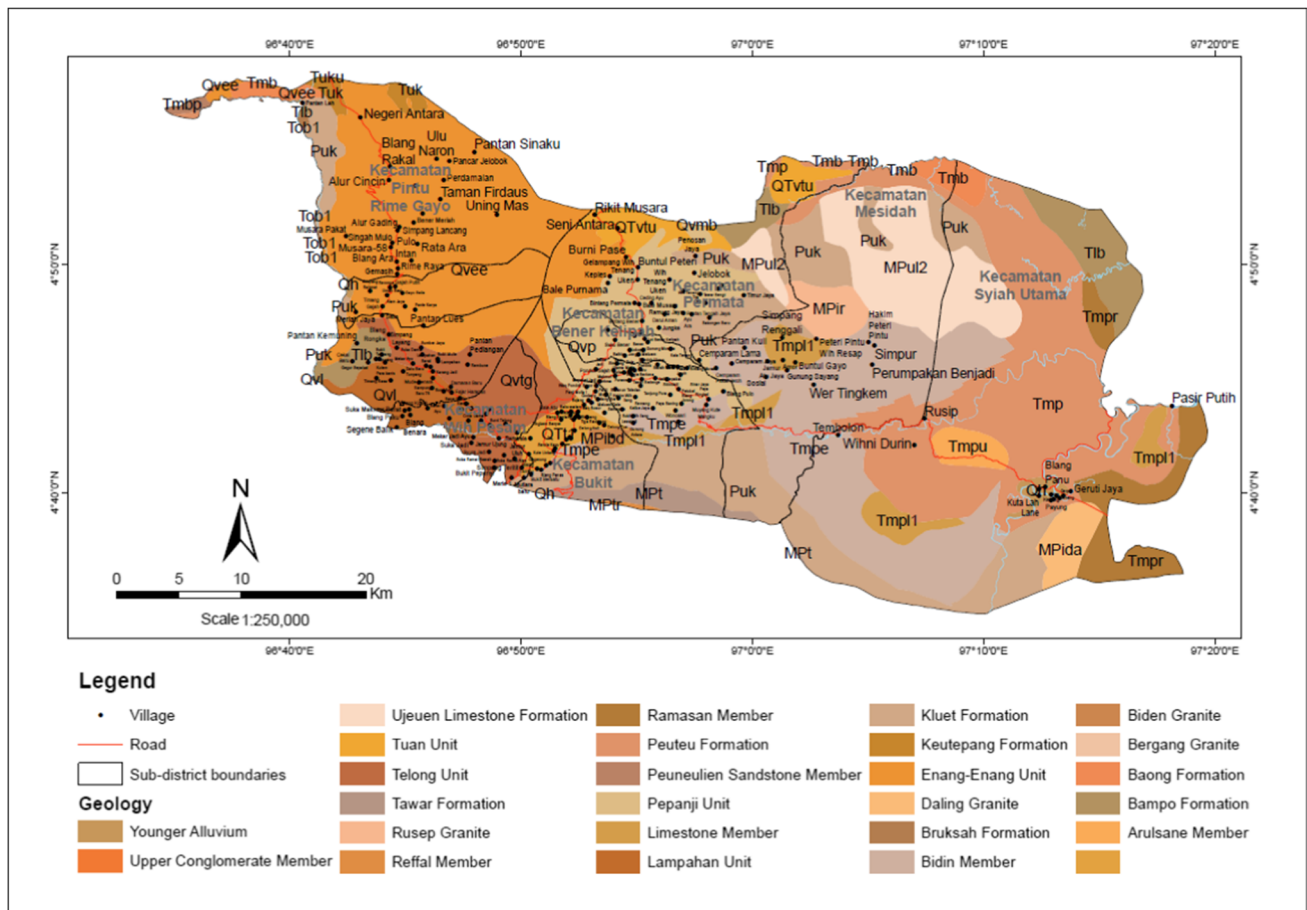


Fig. 6 Geology map for Bener Meriah Sub-district

floor) scores. The geology spatial layer, in polygon format, was divided into the three scores, such as low (volcano, extrusive, intrusive, classic sediments, lava, limestone, and sandstone), high (conglomerates, alluvial fan, neritic), and height (landslides, limestone, river, and litoral). Finally, the fault density spatial data, represented as polygon data (km<sup>2</sup>), classified the density of faults in the region into low (no-fault), medium (less dense with only one fault found in 1000 m buffering), and high (many faults in the area of 1000 m buffering).

### Vulnerability map

Vulnerability map was divided into the social, economic, and physical layers (Fig. 7). Vulnerability is defined as the ratio of exposure to sensitivity, and the exposed assets included human life (social vulnerability), economic territory, and physical structure. Tabular attribute data used in vulnerability analysis were sourced from the BPS databases. All the spatial data were presented by the polygon shapes. The physical vulnerability map was interpreted using Eq. 3,

while the economy vulnerability map was based on Eq. 4. Additionally, the social vulnerability map was calculated using Eq. 5 (Perka BNPB 2/2012) (BNPB 2012).

$$PV = (H * 0.4) + (PF * 0.3) + (CF * 0.3) \tag{3}$$

From Eq. 3, PV is a physical vulnerability, *H* refers to houses, PF denotes public facilities, and CF represents critical facilities.

$$EV = (PL * 0.6) + (PDRB * 0.4) \tag{4}$$

From Eq. 4, EV is an economic vulnerability, PL is a productive land, and PDRB refers to the gross regional domestic product.

$$SV = \left( \frac{\log\left(\frac{PD}{0.01}\right)}{\log\left(\frac{100}{0.01}\right)} * 0.6 \right) + (SR * 0.01) + (PR * 0.01) + (DR * 0.01) + (GAR * 0.01) \tag{5}$$

From Eq. 5, SV, PD, SR, PR, DR, and AGR represent social vulnerability, population density map, sex ratio map,

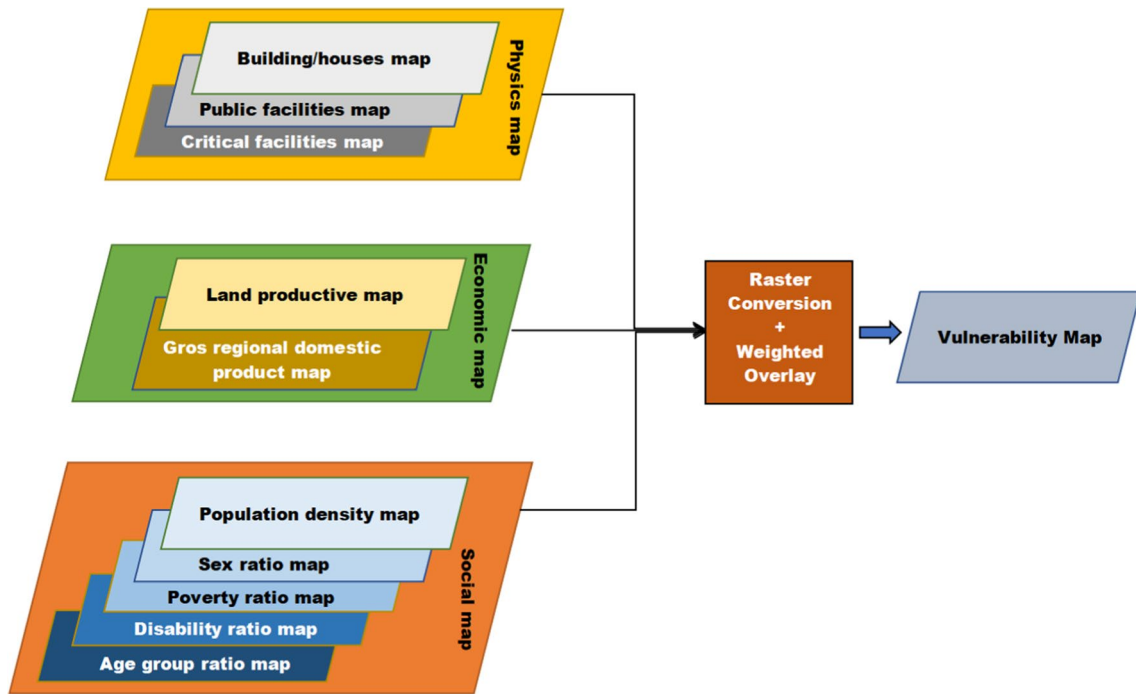


Fig. 7 Preparation of vulnerability map

poverty ratio map, disability ratio map, and age group ratio map, respectively.

Vulnerability map was analyzed by combining physical, economic, and social factors as shown in Eq. 6 (Perka BNPB 2/2012) (BNPB 2012).

$$EVM = (PV * 0.3) + (EV * 0.3) + (SV * 0.4) \tag{6}$$

where EVM is earthquake vulnerability map.

Vulnerability is a condition of a community or society that leads to or causes an inability to deal with disasters. The more “vulnerable” a group of people to disasters, the greater the loss that will be experienced if a disaster occurs in that group of people. Vulnerability analysis is carried out spatially by combining all the constituent components of vulnerability, where each component of vulnerability is also

obtained from the results of the process of combining several constituent parameters.

### Capacity map

Capacity indexes were obtained based on the resilience level of the district at a given time. The district resilience level was the same for all the regions in an area, serving as the lowest scope of this capacity assessment. Therefore, the calculation of the district resilience can be performed simultaneously with the preparation of hazard map in the same area (all spatial data is polygon shaped). The determination of capacity indexes can be made with references to Fig. 8.

Capacity was calculated by assessing the region’s ability to recover from earthquake disaster. Capacity index was derived from the indicators outlined in the Hyogo

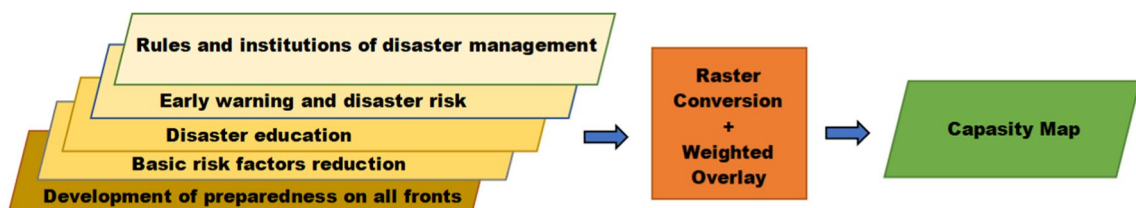


Fig. 8 Preparation of capacity map



Framework for Actions (HFA) (Fariza et al. 2017). Furthermore, it could be divided into five resistance levels based on the indicators of the resilience district achievement:

**Level 1**, a district has taken small actions in disaster risk reduction efforts by implementing some sustainable operations into plans or policies.

**Level 2**, a district implemented some disaster risk reduction efforts with sporadic achievements which resulted in the absence of institutional and systematic policy commitments.

**Level 3**, the government and several communities were committed to disaster risk reduction in a district, and it has been achieved and supported by systematic policy. However, the achievements accomplished with these commitments and policies were not yet sufficient to reduce the negative impacts of disaster.

**Level 4**, the support from the commitment and comprehensive policy on disaster risk reduction in a district has received sufficient achievements. However, there are still some limitations in the commitment, financial resources, or operational capacity affecting the implementation of disaster risk reduction efforts in the area.

**Level 5**, the comprehensive outcomes have been achieved with an adequate commitment and capacity at all the levels of the community and government.

## Results and discussion

### Hazard map

Hazard indexes were arranged based on the parameters of the dataset to assess the possibility of hazard occurring and the magnitude of its impact. This methodology aimed to determine the level of hazard. Subsequently, hazard map was created using GIS, with each component derived from a predefined data source. The data were then divided into three threat classes, namely, low (0.0–0.3), moderate (0.3–0.6), and high (0.6–1).

Figure 9 shows earthquake hazard map for Bener Meriah District, which was analyzed using a scoring analysis method with a raster calculation tool. Analysis involved inserting relevant parameters into Eq. 1 to determine hazard level. The outcome of this assessment indicated that earthquake hazard in Bener Meriah District was at a moderate level, and this was identified in certain sub-districts covering an approximate area of 57,154 ha. The areas include Bandar, Bener Kelipah, Bukit, Gajah Putih, Mesidah, Permata, Pintu Rime Gayo, Syiah Utama, Timang Gajah, and Wih Pesam sub-districts. The highest-level-hazard earthquake was discovered at the Mesidah and Syiah Utama sub-districts with ca. 2059 ha, as shown in Table 2.

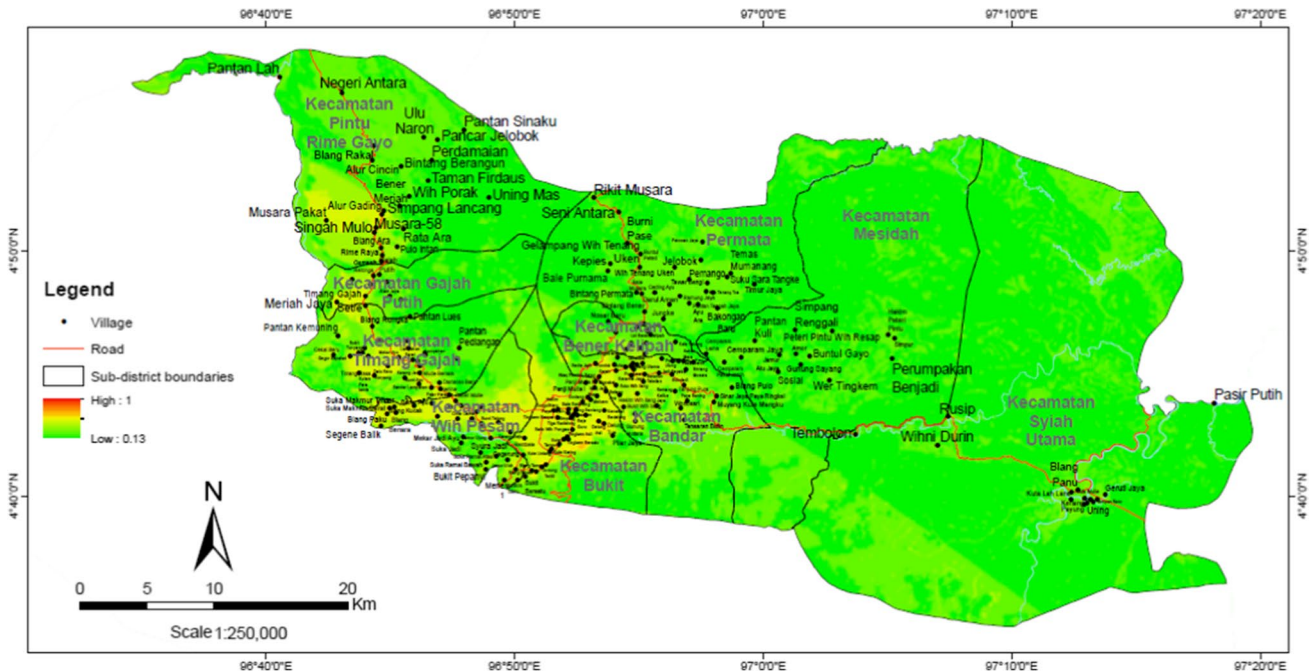


Fig. 9 Hazard map of the Bener Meriah District

**Table 2** Moderate level of earthquake hazard index

Sub-district	Moderate level (ha)	High level (ha)
Bandar	2769.58	-
Bener Kelipah	173.18	-
Bukit	2959.67	-
Gajah Putih	4622.58	-
Mesidah	7338.13	-
Permata	7963.96	-
Pintu Rime Gayo	21,946.17	-
Syiah Utama	4839.86	-
Timang Gajah	4321.51	-
Wih Pesam	21	-
Mesidah	-	1602.30

**Vulnerability map**

Earthquake vulnerability map was analyzed using Eq. 2. The Meusara Pakat village had a high level of vulnerability, while the other settlements had medium and low levels, as shown in Fig. 10 and Table 3.

**Capacity map**

Earthquake capacity map was analyzed using assessment data from Bener Meriah district. Furthermore, the parameters for capacity evaluation consisted of the availability of local policy, local resources, a specific budget, local forums, disaster monitoring systems, early warning devices, and infrastructure for disaster risk reduction. The result showed a high level of capacity for the district, primarily because almost all the assessed parameters were unavailable, as shown in Fig. 11. Only some of capacity parameters were available; hence, map indicated a high score. These results became a reference for the stakeholders, highlighting the need to prioritize the establishment of these parameters in the future. Such measures encompassed local policy, local resources, a specific budget, local forums, disaster monitoring systems, early warning devices, and infrastructure.

**Disaster risk map**

Earthquake disaster risk map was generated by analyzing hazard, vulnerability, and capacity, as outlined in Eq. 1. The

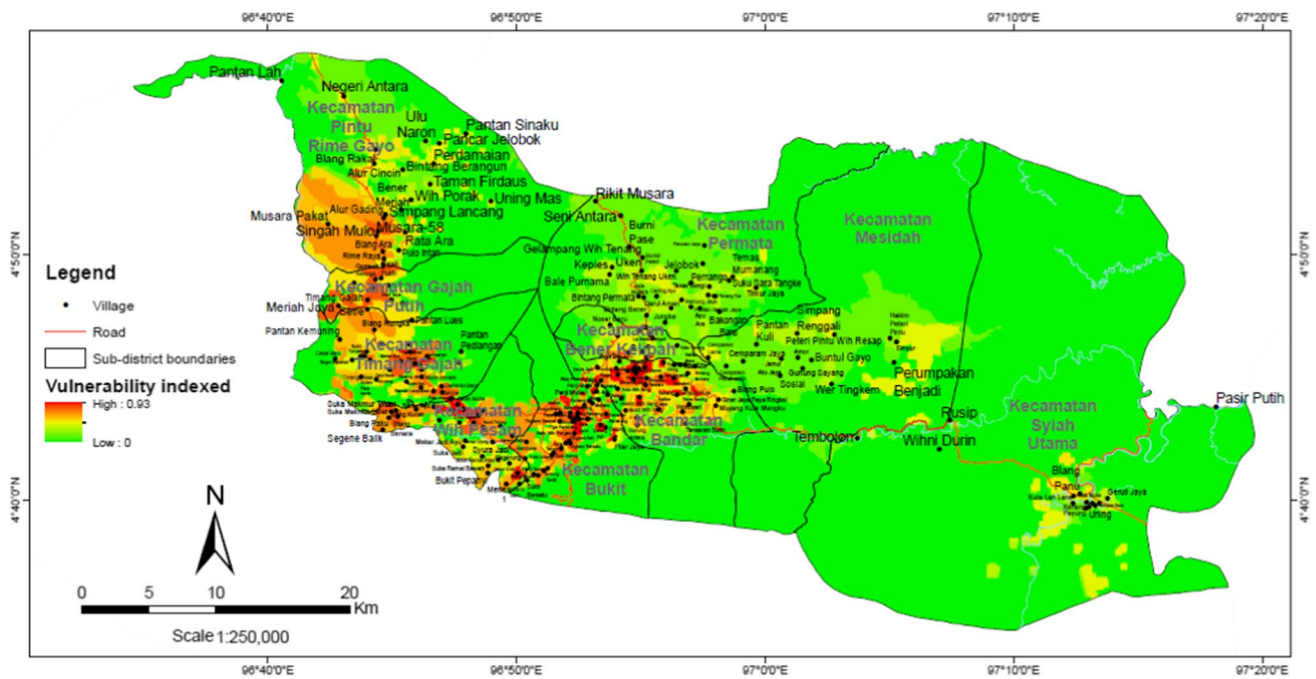


**Fig. 10** Vulnerability map of Bener Meriah District

**Table 3** Vulnerability indexes

Vul. type	Low	Moderate	High
Pop. Exposed (Person)	1976	15	1991
Potential Eco. & Phy. Losses	IDR 1077024853770	IDR 9850998017	IDR 1086875851787
Potential Envir. Losses (ha)	32,005	2059	34,064

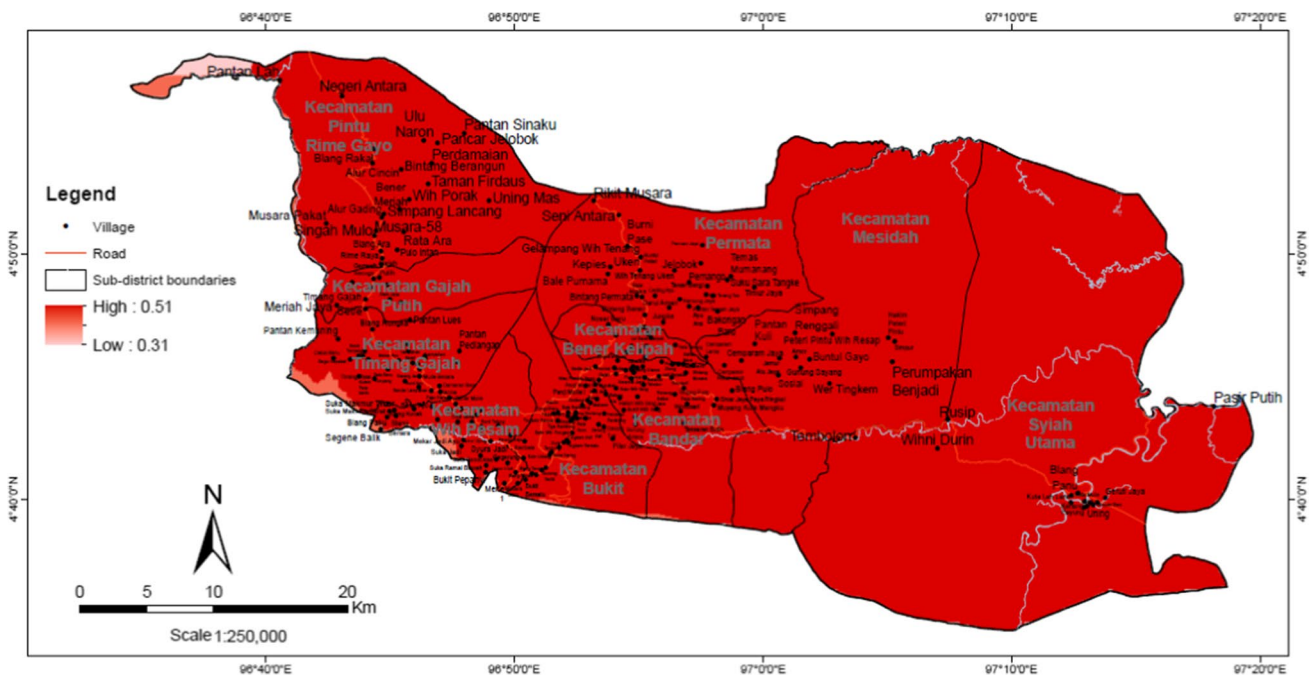


Fig. 11 Capacity map of Bener Meriah District

obtained results showed that disaster risk level for Meusara Pakat village was high, while for other settlements, it varied between medium and low, respectively, as presented in Fig. 12, Table 4, and Table 5.

In 11 sub-districts, earthquakes categorized as low risk have exposed an estimated 122 people and potentially threatened 37,768 in vulnerable groups, thereby leading to economic-physical losses of about IDR 368 billion. Disaster risk in the medium category has resulted in the exposure of 1869 people, physical losses of about IDR 718 billion, and threatened 48,809 people in vulnerable groups.

Disaster risk map was a tool to assess the possibility and number of losses due to the existing hazard. By understanding the likelihood and magnitude of losses, the focus on planning and integrating the implementation of disaster management becomes more effective. Disaster risk map was the basis for ensuring the alignment and effectiveness of regional disaster management (Farhan and Akhyar 2017). The Bener Meriah District disaster risk map was constructed through an overlay of hazard, vulnerability, and capacity map, using Eq. 1. For example, in this study, the Bandar sub-district had the highest number of exposed people at risk (Fig. 12 and Table 5). This was attributed to the larger population of people with disabilities, the elderly, and children living in the sub-district. Meanwhile, the sub-district with the highest property losses in IDR currency was Pintu Rime Gayo District, mainly due to the concentration of the downtown area in this region. The presented disaster map can support the stakeholders from the Bener Meriah District

to make strategic planning and decisions on disaster mitigation or make quick actions when earthquake occurs.

This method of creating disaster map required high accuracy to produce more accurate output data. The study does have some limitations that need to be addressed. Spatial data used for hazard map analysis, including PGA, distance to the active faults, MMI, geomorphology, geology, and fault density, was available at a scale of 1:250,000 and was produced by the Ministry of Public Works, Energy, and Mineral Resources, the Geospatial Information Bureau, the Geology Bureau, the Bureau of Meteorology, Climatology, and Geophysics. However, no detailed scale data were available at the time of this study. Those spatial data were interpolated using GIS tools (Sun et al. 2007; Jena et al. 2020). Despite these limitations, the method used can serve as a reference for generating large-scale disaster map, such as those for districts, provinces, and national areas. Furthermore, this method can be adapted for creating small-scale disaster map starting from city, village, and sub-district, when relevant ministries possess PGA, distance to the active faults, MMI, geomorphology, geology, and fault density spatial data (Gupta and Satyam 2022; Hegazi et al. 2023). In order to thoroughly investigate the macroseismic intensity on the Modified Mercalli Intensity (MMI) scale, which is based on ground motion engineering characteristics such as peak ground acceleration (PGA), deduced from ground motion, the described isoseismal maps were constructed. Bener Meriah District’s motion damping properties (Pailoplee 2012). The MMI value becomes a linear function in

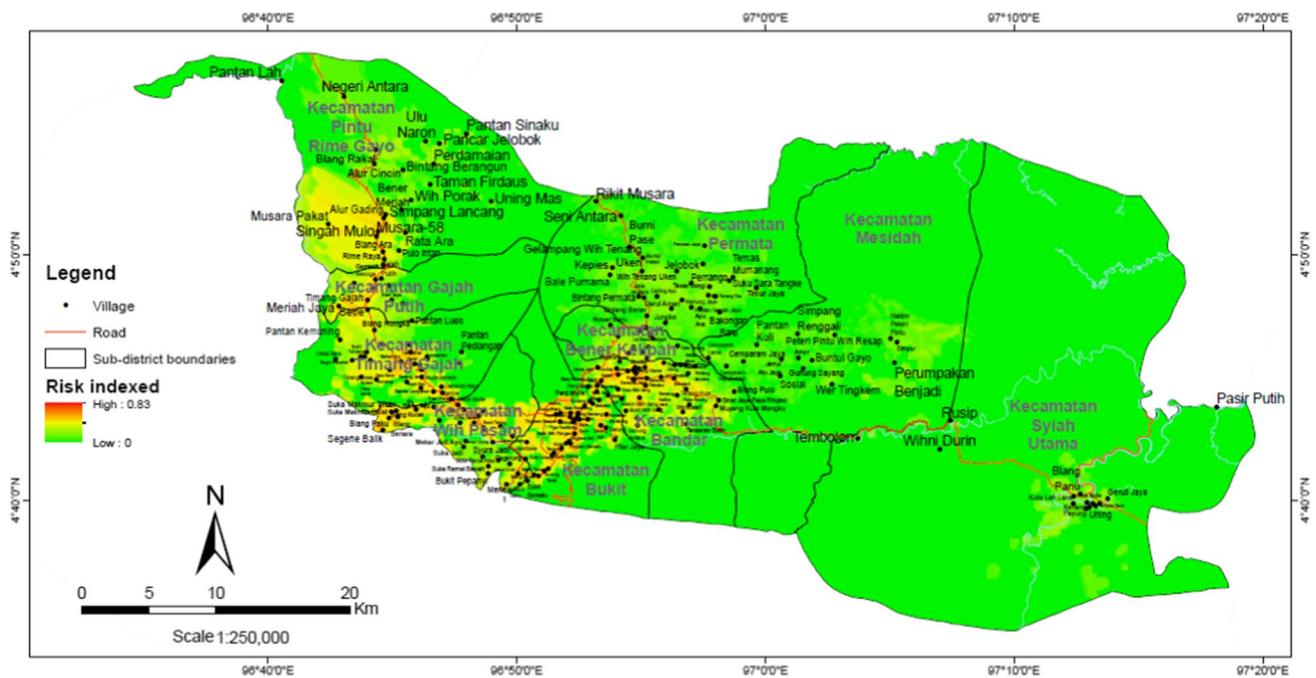


Fig. 12 Disaster map of Bener Meriah District

**Table 4** Earthquake disaster risk with the low category (people)

Sub-district	Exposed people	Poverty	Disabled	Elderly	Toddler	Potential Losses (IDR)
Bandar	15	1029	29.00	1673	1673	24,396,212,295
Bener Kelipah	1	17	-	18	18	6,678,338
Bukit	35	2248	129	5490	5490	100,135,251,815
Gajah Putih	7	690	32	1795	1795	65,403,680,442
Mesidah	11	676	7	545	545	20,165,656,037
Permata	12	1276	46	1927	1927	58,009,578,864
Pintu Rime Gayo	8	508	20	691	691	35,872,468,329
Syiah Utama	22	351	22	519	519	8,359,045,955
Timang Gajah	10	1244	31	1848	1848	55,953,279,168
Wih Pesam	1	94	3	152	152	375,363,922
<b>Total</b>	<b>122</b>	<b>8133</b>	<b>319</b>	<b>14,658</b>	<b>14,658</b>	<b>368,677,215,165</b>

**Table 5** Earthquake disaster risk with the moderate category (people)

Sub-district	Exposed people	Poverty	Disabled	Elderly	Toddler	Potential losses (IDR)
Bandar	988	1938	91	4153	4153	93,632,672,045
Bener Kelipah	1	11	-	32	32	1,226,225,339
Bukit	27	562	44	1554	1554	28,724,038,860
Gajah Putih	8	783	37	2243	2243	108,322,440,191
Mesidah	6	303	17	539	539	19,886,747,850
Permata	621	1812	58	2544	2544	120,750,202,671
Pintu Rime Gayo	33	3315	124	4434	4434	270,347,891,801
Syiah Utama	3	55	7	122	122	2,364,818,414
Timang Gajah	13	1757	29	2273	2273	64,203,966,873
Wih Pesam	170	387	21	835	835	8,739,632,578
<b>Total</b>	<b>1870</b>	<b>10,923</b>	<b>428</b>	<b>18,729</b>	<b>18,729</b>	<b>718,198,636,622</b>

**Table 6** Technical team in the Bener Meriah District

No	Institution	Number of representatives
SKPD/government bodies (Dinas)		
1	Regional Disaster Management Agency (BPBD)	3
2	Regional Development Planning Agency (BAPPEDA)	2
3	Mineral Resources Energy (ESDM)	1
4	Firefighter (DAMKAR)	2
5	Forestry and Plantation Service (DISHUTBUN))	1
6	Volcano Monitoring Post (PPGA)	1
7	<i>Bina Marga Cipta Karya (BMCK)</i>	2
8	Regional SAR Agency (BASARDA)	1
9	Department of Health (DINKES)	1
10	National Family Planning Coordinating Agency and Women's Empowerment (BKKBN and PP)	1
11	Social Service (DINSOS)	1
12	Department of Transportation, Communication and Telematics (DISHUBKOMINTEL)	1
Non-governmental institution		
13	RAPI	1
14	PMI	1
15	NGO/Karst Aceh	1
16	Media	1
Private Sector		
17	Bener Meriah Coffee Association	1
University		
18	Gajah Putih University	1
Community		
19	Disaster Preparedness Communication Forum (FKSB)	1
20	Gayo Traditional Council (MAG)	1
TOTAL		25

relation to  $\log_{10}$  (PGA), where MMI is the macroseismic intensity level on the MMI scale and PGA is the peak ground acceleration ( $\text{cm/s}^2$ ).

### Focus group discussion report

Mapping disaster risk was implemented through the five main activities which included the technical team initial meeting, formal coordination for data clarification, technical team meetings, public seminary, and disaster risk map finalization. Disaster Management Plan (DM Plan) Development, was implemented through five main activities which included the technical team initial meeting, technical team meetings (three times meeting), public seminary, technical team meeting to finalize the DM plan, and the DM plan advocacy and socialization. To achieve the production of disaster risk map and disaster management plan, it is essential to involve stakeholders, particularly the technical team (Gu et al. 2023 and Anshori et al. 2022). This involvement ensures the understanding established during the mobilization phase is upheld

and that team research gives priority to engaging relevant actors and stakeholders, as mandated by BNPB (the Indonesian disaster management agency). The focus will be on hazard and threats that require attention. For the technical team members' participation, their involvement needs to be officially confirmed through the Decree of Bupati (District Regent) or the District Secretary (Sekda).

The BNPB emphasized the importance of accommodating a diverse range of actors/stakeholders in the development of both documents including the government bodies (Dinas), non-governmental organizations, mass media, community, private entities, and universities/colleges. The institutions that will be involved in this process are listed in Table 6.

### Conclusion

In conclusion, a comprehensive analysis was conducted on earthquake hazard, vulnerability, capacity, and disaster risk analysis for Bener Meriah district. A three-level risk

assessment method (high, medium, and low) was effectively used in conjunction with GIS technology to assess earthquake disaster risks in the area. Through spatial analysis using scoring and overlay techniques, disaster risk was categorized into two main classifications, namely, medium and low. The low-risk category was determined based on specific criteria, including 122 people exposed, 37,768 under threat, and economic-physical losses of IDR 368 billion. Meanwhile, the medium-risk category encompassed 1869 people exposed, about 48,809 potentially vulnerable and under threat, and total economic-physical losses of IDR 718 billion. Among all the locations, Meusara Pakat village was identified as having the highest risk for earthquake disaster according to the scoring data for hazard, vulnerability, and capacity.

**Data Availability** The data used in this study is proprietary in nature and cannot be made available.

## Declarations

**Conflict of interest** The author(s) declare that they have no competing interests.

## References

- Abdelkarim B, Telahigue F, Agoubi B (2022) (2022) Assessing and delineation of groundwater recharge areas in coastal arid area southern Tunisia. *Groundw Sustain Dev* 18:100760. <https://doi.org/10.1016/j.gsd.2022.100760>
- Abdelkarim B, Telahigue F, Aabaab N, Boudabra B, Agoubi B (2023) AHP and GIS for assessment of groundwater suitability for irrigation purpose in coastal-arid zone: Gabes region, southeastern Tunisia. *Environ Sci Pollut Res* 30:15422–15437. <https://doi.org/10.1007/s11356-022-23193-4>
- Agoubi B, Kharroubi A (2019) Groundwater depth monitoring and short-term prediction: applied to El Hamma aquifer system, south-eastern Tunisia. *Arab J Geosci* 12:324. <https://doi.org/10.1007/s12517-019-4490-1>
- Anshori RM, Samodra G, Mardiatno D, Sartohadi J (2022) Volunteered geographic information mobile application for participatory landslide inventory mapping. *Comput Geosci* 161. <https://doi.org/10.1016/j.cageo.2022.105073>
- BNPB (2012) Peraturan Kepala Badan Nasional Penanggulangan Bencana Nomor 02 Tahun 2012 Tentang Pedoman Umum Pengkajian Risiko Bencana [Perka BNPB 2/2012: Regulation of the Head of the National Disaster Management Agency Number 02 of 2012 About General Guidelines for Disaster Risk Assessment]. Indonesia. Accessed 10 August 2022. <https://bnpb.go.id/uploads/migration/pubs/30.pdf>
- Chang-chun L, Guang-sheng Z, Tian-jie L, A-du G (2011) Quick image-processing method of UAV without control points data in earthquake disaster area. *Trans Nonferrous Met Soc China* 21:s523–s528
- Ezzelarab M, Shokry MMF, Mohamed AME, Mohamed AA, El-Hadidy MS (2016) Evaluation of seismic hazard at the northwestern part of Egypt. *J Afr Earth Sc* 113:114–125
- Farhan A, Akhyar H (2017) Analysis of tsunami disaster map by geographic information system (GIS): Aceh Singkil-Indonesia”, *IOP Conf. Series: Earth and Environmental Science* 56:1–13
- Fariza A, Rusydi I, Hasim JAN, Basofi A (2017) Spatial flood risk mapping in east Java, Indonesia, using analytic hierarchy process - natural breaks classification, 2nd International conferences on Information Technology, Information Systems and Electrical Engineering (ICITISEE). Yogyakarta 2017:406–411
- Feng X, Xuping C, Aizhu R, Xinzheng L (2008) Earthquake disaster simulation for an urban area, with GIS, CAD, FEA, and VR integration. *Tsinghua Sci Technol* 13(S1):311–316
- Gaspar-Escribano JM, Rivas-Medina A, Parra H, Cabañas L, Benitoa B, Barajas SR, Solares JMM (2015) Uncertainty assessment for the seismic hazard map of Spain. *Eng Geol* 199:62–73
- Gu E, Meng T, Wang H, Zhang A (2023) E-government use, perceived transparency, public knowledge of government performance, and satisfaction with government: an analysis of mediating, moderating, and framing mechanisms based on the COVID-19 outbreak control survey data from China. *Soc Indic Res* 169:79–124. <https://doi.org/10.1007/s11205-023-03135-4>
- Gupta K, Satyam N (2022) Estimation of Arias intensity and peak ground acceleration (PGA) using probabilistic seismic hazard assessment of Uttarakhand state (India). *Arab J Geosci* 15:437. <https://doi.org/10.1007/s12517-022-09733-9>
- Halvorson SJ, Hamilton JP (2010) In the aftermath of the Qa'yamat: 1 the Kashmir earthquake disaster in northern Pakistan. *Disasters* 34(1):184–204
- Hegazi AM, El-Rayes AE, Arnous MO, Al-Moazamy AA (2023) Revealing the geomorphic parameters of neotectonics based on geological and seismic data at Wadi Beda basin, NW Gulf of Suez. *Egypt Arab J Geosci* 16:82. <https://doi.org/10.1007/s12517-022-11165-4>
- Hutchings SJ, Mooney WD (2021) The seismicity of Indonesia and tectonic implications. *Geochem Geophysics Geosyst* 22(9):1–42. <https://doi.org/10.1029/2021GC009812>
- Jena R, Pradhan B, Beydoun G et al (2020) Seismic hazard and risk assessment: a review of state-of-the-art traditional and GIS models. *Arab J Geosci* 13:50. <https://doi.org/10.1007/s12517-019-5012-x>
- Kimura R, Inoguchi M, Tamura K, Hayashi H (2015) Comparison between the life recovery processes after the Mid-Niigata Earthquake and the Chuetsu-Oki Earthquake-Results of a random sampled social survey using the life recovery calendar and GIS-based spatiotemporal analysis. *J Disaster Res* 10(2):196–203
- Missaoui R, Abdelkarim B, Ncibi K, Hamed Y, Choura A, Essalami L (2022) Assessment of groundwater vulnerability to nitrate contamination using an improved model in the Regueb Basin. *Cent Tunis Water Air Soil Pollut* 233:320. <https://doi.org/10.1007/s11270-022-05806-3>
- Missaoui R, Ncibi K, Abdelkarim B, Bouajila A, Choura A, Hamdi M, Hamed Y (2023) Assessment of hydrogeochemical characteristics of groundwater: link of AHP and PCA methods using a GIS approach in a semi-arid region. *Cent Tunis Euro-Mediterr J Environ Integr* 8:99–114. <https://doi.org/10.1007/s41207-023-00345-7>
- Pailoplee S (2012) Relationship between Modified Mercalli Intensity and peak ground acceleration in Myanmar. *Nat Sci* 4:624–630. <https://doi.org/10.4236/ns.2012.428082>
- Rahman N, Ansary MA, Islam I (2015) GIS based mapping of vulnerability to earthquake and fire hazard in Dhaka city, Bangladesh. *Int J Disaster Risk Reduction* 13:291–300
- Rürup and Charlin A (2017) Strengthening capacities for the use of GIS in disaster risk reduction, thesis student Division of Risk Management and Societal Safety, Lund University

- Sun C, Chun S, Ha T, Chung C, Kim D (2008) Development and application of a GIS-based tool for earthquake-induced hazard prediction. *Comput Geotech* 35(3):436–449. <https://doi.org/10.1016/j.compgeo.2007.08.001>. (ISSN 0266-352X)
- Uitto JI (1998) The geography of disaster vulnerability in megacities: a theoretical framework. *Appl Geogr* 18(1):7–16
- Urakawa G (2016) Building a GIS-based information system with seamless interaction between operations and disaster management - new challenges of Kitakyushu Fukuoka in Using Spatial Information for Regional Disaster Resilient Societies. *J Disaster Res* 11(5):897–910
- Wardhana BAS, Hafizh I, Arsyi H, Faridsyah WA, Marom N (2023) Exploring the overlooked seaurala potential in Arun field; a preliminary study from outcrops and subsurface data in North Sumatra Basin. Proceedings, Indonesian Petroleum Association, Forty-Seventh Annual Convention & Exhibition, July 2023
- Yanto, Apriyono A, Santoso PB, Sumiyanto (2022) Landslide susceptible areas identification using IDW and Ordinary Kriging interpolation techniques from hard soil depth at middle western Central Java, Indonesia. *Nat Hazards* 110:1405–1416. <https://doi.org/10.1007/s11069-021-04982-5>
- Ye M, Wang J, Huang J, Xu S, Chen Z (2012) Methodology and its application for community-scale evacuation planning against earthquake disaster. *Nat Hazards* 61:881–889
- Yeh H-F, Hsu H-L (2019) Using the Markov chain to analyze precipitation and groundwater drought characteristics and linkage with atmospheric circulation. *Sustainability* 11(6):1817. <https://doi.org/10.3390/su11061817>
- Zook M, Graham M, Shelton T, Gorman S (2010) Volunteered geographic information and crowdsourcing disaster relief: a case study of the Haitian Earthquake. *World Med Health Policy* 2(2):7–33
- Springer Nature or its licensor (e.g. a society or other partner) holds exclusive rights to this article under a publishing agreement with the author(s) or other rightsholder(s); author self-archiving of the accepted manuscript version of this article is solely governed by the terms of such publishing agreement and applicable law.